Monitoring Ground Subsidence in Shanghai Maglev Area Using PALSAR and ASAR Data

Jicang Wu *, Lina Zhang, Tao Li

Department of Surveying and Geo-Informatics, Tongji University, Shanghai, China - jcwu@tongji.edu.cn

KEY WORDS: Shanghai maglev, ground subsidence, SBAS, ALOS, PALSAR, LOS velocities

ABSTRACT:

Shanghai maglev is a very fast traffic tool, so it is very strict with the stability of the roadbed. However, the ground subsidence is a problem in Shanhai because of the poor geological condition and some human-induced factors. So it is necessary to monitor ground subsidence in the area along the Shanghai maglev precisely and frequently. Traditionally, precise levelling method is used to survey along the track. It is expensive and time consuming, and can only get the ground subsidence information on sparse benchmarks. Recently, small baseline differential SAR technique comes into playing a valuable part in monitoring of ground subsidence, which can extract ground subsidence information in a wide area and with high spatial resolution. In this paper, L-band ALOS PALSAR data and C-band ENVISAT ASAR data are used to extract ground subsidence information using SBAS method in Shanghai maglev area. The results show that the general pattern of ground subsidence from InSAR processing of two differential bands of SAR images is similar. Both results show that there is no significant ground subsidence on the maglev line. Near the railway line, there are a few places with significant local subsidence rates at about -20mm/y or even more, such as Chuansha town, the junction of the maglev and Waihuan road.

1. INTRDUCTION

Shanghai maglev is the first successful commercial maglev transportation system in the world. Since 2005, Shang maglev has normally given commercial service to public. The whole length of Shanghai maglev is 36km and the maximum running speed is 403km/h. As a kind of very fast traffic tools, the running of Shanghai maglev requires a stable ground support bases. However, the ground subsidence in Shanghai is a problem because of the poor geological condition and some human-induced factors. Nowadays, the average annual subsidence velocity is nearly 10mm/y in the centre downtown[1]. So it is very important for detection of potential ground subsidence near the railway to ensure the safety of the maglev line. However, spirit levelling is very time consuming and laborious. Recently, differential synthetic aperture radar interferometry (DInSAR) technology offers a convenient and efficient method for monitoring ground subsidence.

DInSAR is a new technique for earth observation, with features of large-scale (100km × 100km), high spatial resolution (20m × 20m), high accuracy (mm level)[2]. DInSAR is widely used in the field of earth sciences such as seismic default, ground subsidence, volcanic activity, land slide and so on[3][4][5]. As a kind of very slow deformation, ground subsidence is easy to be affected by the phase decorrelation and atmospheric inhomogeneities[6] if using DInSAR method. The emergence of time series analyzing method provides a new idea to solve these problems. The time-series processing concentrates on those points called coherent targets[7] that maintaining good coherence even during a long observation interval. There are many methods of time series analysis in the application of DInSAR. In this paper, we choose small baseline subsets(SBAS) [8][9]method which based on different master images for DInSAR. SBAS divides the SAR images of the same region into several subsets. The interferometric baselines are small in each subset, but bigger than critical baseline between every two subsets. By filtering and other method, the influence of atmospheric delay and topographic height can be removed. Then we can use SVD decomposition to get the mean velocity in Line of Sight.

In this paper, L-band ALOS PALSAR data and C-band ENVISAT ASAR data are used to extract ground subsidence information in Shanghai maglev area. At first, basic rational of the SBAS algorithm is introduced. Then 17 scenes of ALOS PALSAR 1.0 data and 27 scenes of ASAR SLC data are used for taking InSAR processing respectively. The results show that the general pattern of ground subsidence from InSAR processing of two differential bands of SAR images is similar. Both results show that most places of the maglev area have no significant ground subsidence. There are a few places with significant local subsidence rates at about -20mm/y or even more, such as Chuansha town, the junction of the maglev and Waihuan road, and so on.

2. BASIC RATIONAL OF THE SBAS ALGORITHM

DInSAR uses the phase difference information of two complex radar images to determine the small deformation of ground targets [10]. The observed interferometric phase difference can be written as follows [11]:

$$\phi = \phi_{def} + \phi_{topo} + \phi_{orb} + \phi_{trop} + \phi_{noise} \qquad (1)$$

where ϕ_{def} is the phase related to surface motion, ϕ_{topo} is the topographic phase corresponding to curve surface of the earth and ground elevation, ϕ_{orb} is the phase caused by orbit errors,

* Corresponding author.

ϕ_{trop} is the phase related to atmospheric delay, and ϕ_{noise} is random noise due to other reasons.

For two-pass DInSAR, external DEM data should be used to remove the topographic phase. ASTER GDEM products are used in this paper. The spatial resolution of ASTER GDEM is about 30m and vertical accuracy is about 20m in flatten area such as Shanghai. The phase error caused by DEM errors can be expressed as [12]

$$\sigma_{\phi_{dem}} = -\frac{4\pi B_{\perp}}{\lambda R \sin\theta}\sigma_{dem} \tag{2}$$

From this formula we can see long perpendicular baseline will introduce more topographic errors, and only images with short baseline are used to take interferometry, so as to weaken DEM influences. By equation (2), topographic errors can be removed if we know errors in height.

The atmospheric delay may result in great error in InSAR results. There is currently no promising way to eliminate the influence entirely from the interferograms. As the atmospheric error is correlated in space but uncorrelated in time, most part of the influences can be reduced using filtering. Moreover, the orbit errors influences can be reduced using a polynomial fitting method. We suppose that the deformation between the two SAR images is very small so that it can be ignored to some extent. Then the phase can be expressed as:

$$\phi = \phi_{def} + \phi_{noise} \tag{3}$$

Suppose we have N interferometric pairs, phase ϕ_i is acquired between two SAR images with time interval t_i (in unit of year), and then the phase rate v_i can be expressed as:

$$v_i = \frac{\phi_i}{t_i} \tag{4}$$

Suppose the surface deformation is linear, a model can be formed:

$$\phi_i = \bar{v} \cdot t_i + \phi_{noise} \tag{5}$$

To get credible results, the point of high coherence is chosen for stacking. Define average coherence coefficient of a point as:

$$\overline{\gamma} = \frac{1}{N}\sum_{i=1}^{N}\gamma_i \tag{6}$$

Where γ_i is the coherence coefficient of the point in the i-th interferogram. In practice, a threshold is set and the points will be used for the stacking method only when its average coherence coefficient, $\overline{\gamma}$, is larger than the given threshold.

To the selected point for stacking, setting their coherence coefficient as the weight in the least squares estimation of (5), then the phase rate is obtained as:

$$\bar{v} = \sum_{i=1}^{N}\gamma_i \cdot \phi_i \cdot t_i \Big/ \sum_{i=1}^{N}\gamma_i \cdot t_i^{\,2} \tag{7}$$

Equation (7) will be applied for determining deformation rate of ground point in the following

3. SURFACE DEFORMATION ANALYSIS

Shanghai is one of the biggest cities that suffering ground subsidence disaster in China. The deformation started since 1921 and the settlement came to 1.6m till 1965 because of over extracting of groundwater, which seriously impeded the city construction such as subway and large buildings. With some effective procedures after 2000, the subsidence velocity in downtown city have been under the control of 20 mm/y[1]. Currently the average deformation velocity is 10mm/y[13], which can be simulated as a kind of linear movement.

Ground subsidence has a regional moving trend, so it is not sufficient to observe only along the railway line. In this paper, we choose the area 10 km away from the maglev line in order to detect the potential ground subsidence area. The red line stands for the maglev line in Figure 1.

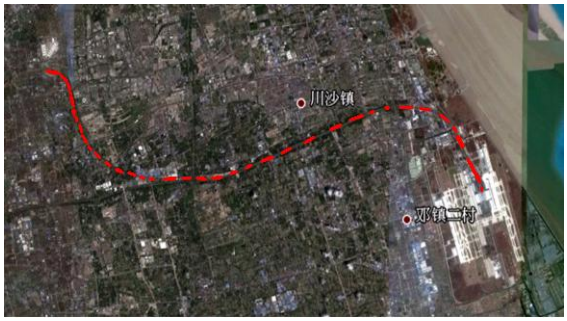

Figure 1. Experiment area

3.1 ENVISAT data processing

Two kinds of data -Envisat and ALOS are used in this paper. Firstly, 27 scenes of Envisat ASAR SLC data between 2007 and 2010 are used for making InSAR processing. Taking into account that the time interval is small, we ignore the time baselines. The vertical baseline of Envisat ASAR inteferograms are less than 180m. The baselines of all interferograms are listed in Figure 2.

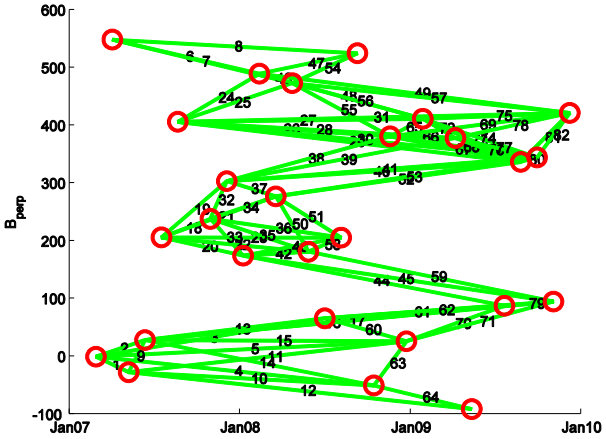

Figure 2. The baseline combination of Envisat data

In Figure 2, the horizontal axis is time, in days, and the vertical axis is the length of vertical baseline, in m. With the combination of Figure 2, 82 interferogtams are generated with ASAR data, shown in Figure 3.

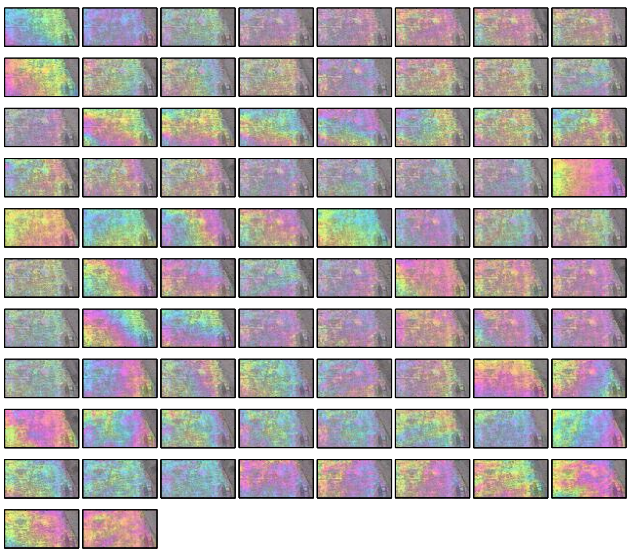

Figure 3. Interferograms of ENVISAT

In Figure 3, it can be seen that the color of the interferograms of ENVISAT change rapidly, the difference of the phase value in some interferograms even exceeds more than a cycle, indicating that the interferograms are significantly affected by atmospheric phase delay errors.

Using the SBAS methods, the subsiding velocities of the target points in the line of sight are extracted and shown in Figure 4.

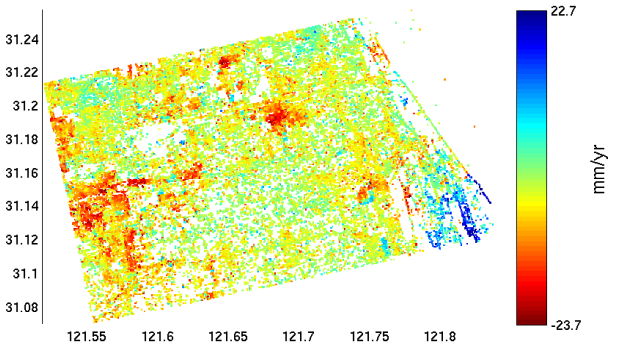

Figure 4. Envisat result

From Figure 4, it can be seen that the distribution of coherent targets is uniform, and LOS velocities are between -23.7-22.7 mm/y, where negative sign indicates the settlement. In the study area of about 500 km^2, totally 28290 coherent targets are obtained, and the point density reached 57 per square kilometre. It can be seen from the figure, there is a large irregular subsidence belt near the starting part of the maglev line. Meanwhile, there are two funnel-shaped settlements near the maglev line, one is in the junction of the maglev and Waihuan road, the other lies in Chuansha town. Overall, the subsidence condition of Shanghai maglev line is better than the surroundings which suffering ground subsidence at a speed of more than 20mm/y.

3.2 ALOS data processing

ALOS data we used belong to two kinds of mode: one is FBS, the other is FBD. The two modes of data have no significant difference in interference effect. FBS data is resampled to have the same range resolution with FBD. Between 2007 and 2010, 18 scenes of ALOS PALSAR 1.0 data are used for taking InSAR processing. With the vertical baseline is limited to 800m, the vertical baselines of interferograms are shown in Figure 5.

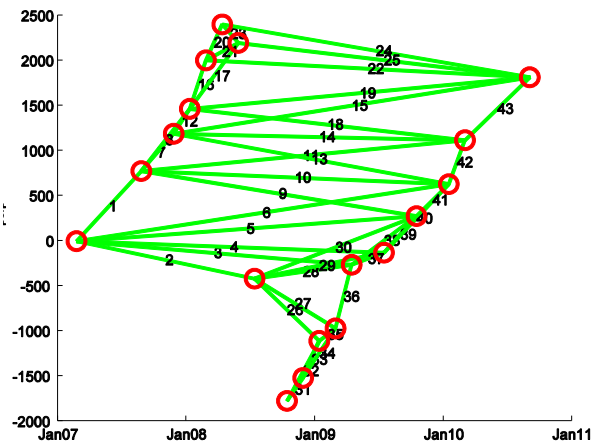

Figure 5. Baseline combination of ALOS PALSAR data

In Figure 5, the horizontal axis is time, in day, vertical axis is the length vertical baseline, in metre. Following the combination of Figure 5, 43 interferogtams are obtained with PALSAR data, showing in Figure 6.

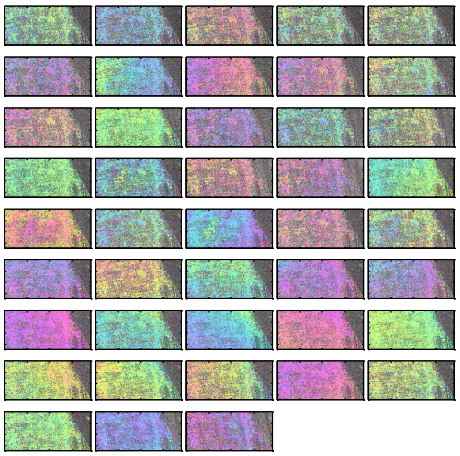

Figure 6. Interferograms of ALOS data

From Figure 6, it can be seen that the interference are relatively smooth, and phase changes are not more than one cycle, indicating that atmospheric phase delay errors on the interference effect is not significantly. Then using the above described SBAS method, average velocities in the line of sight of the target points are obtained and shown in Figure 7.

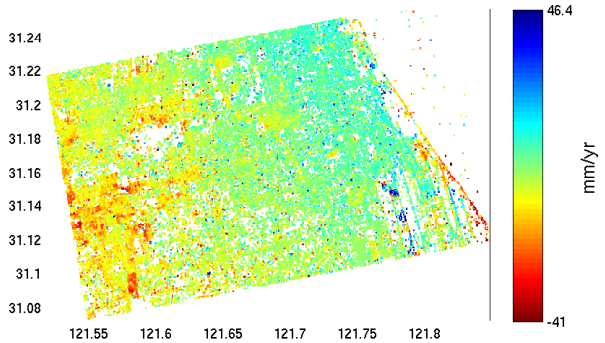

Figure 7. LOS velocities of ALOS

In the study area, totally 28290 coherent targets are chosen in about 500 km2 zone. From Figure 7, it can be seen that the coherent targets are well distributed, and LOS velocities changes from -41 to 46.4 mm/y. A big irregular subsidence belt appears near the starting part of the maglev line. In Chuansha town, there is a little funnel-shaped settlement as well. It must be pointed out that there are singular points which are much different from the surrounding points in Figure 7. Such as a large uplift blue point mixed in the middle of a settlement area, which may due to that selected targets are not reliable.

3.3 Results comparing and analysing

Both LOS velocities of ALOS and ENVISAT are relative values, referring to the same reference area. In order to compare the both velocity results, histograms of both velocity results are shown in Figure 8 and Figure 9.

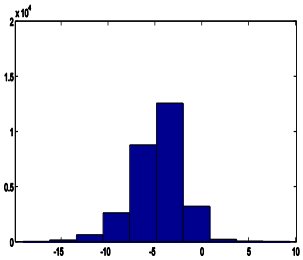

Figure 8. Statistics of Envisat

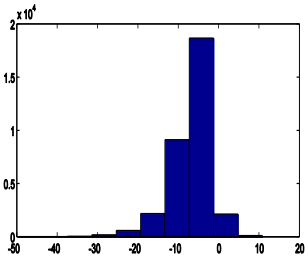

Figure 9. Statistics of ALOS

In Figure 8 and Figure 9, the shape of both histograms is very similar to each other, and the subsidence rate on most points is between -10 and 0 mm/y. The histogram of Envisat data is evenly segmented, and has more information in details. The histogram of ALOS data is a bit precipitous and the maximum value is twice bigger than Envisat data, which maybe the different look angle and other different parameters. According to LOS velocities of ALOS in Figure 7, there are some points with large uplift speed mixed in the middle of a settlement area. These error points are brought by some unreliable points, partly because the number of ALOS images is not sufficient.

By a sequence of spatial and time filtering, atmospheric phase are extracted from both SAR data showing as following.

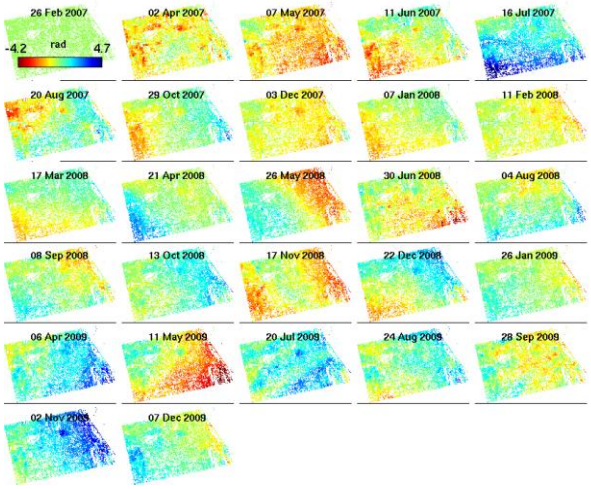

Figure 10. atmosphere phase difference from Envisat data

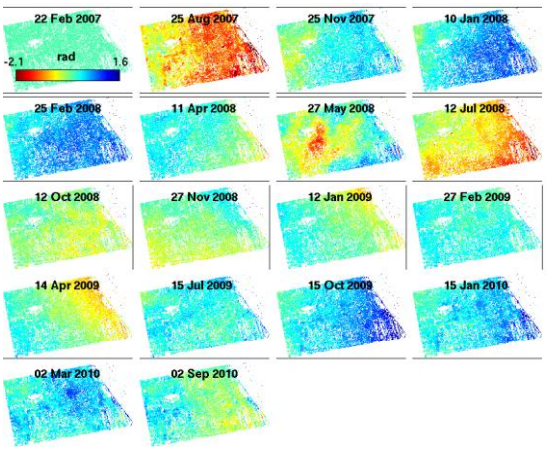

Figure 11. atmosphere phase difference from ALOS data

Figure 10 stands for atmosphere phase difference between master and slave data from Envisat data; Figure 11 stands for atmosphere phase difference between master and slave data from ALOS data.

Comparing with ALOS data, Envisat data is tend to be influenced by atmospheric delay. This may be caused by that the wave length of ALOS PALSAR is longer than ENVISAT ASAR. As microwave travelling through the atmosphere, the longer the wave length is, the weaker the atmosphere delay is.

4. CONCLUSION

In this paper, L-band ALOS PALSAR data and C-band ENVISAT ASAR data are used to extract ground subsidence information in Shanghai maglev area. The results show that the general pattern of ground subsidence from InSAR processing of two differential bands of SAR images is similar. Both results show that there is no significant ground subsidence on the maglev line. Near the railway line, there are a few places with significant local subsidence rates at about -20mm/y or even more. For example, a big irregular subsidence belt appears near the starting part of the maglev line, especially near the junction of the maglev and Waihuan road. There is also a little funnel-shaped settlement in Chuansha town.

From the velocities results, it can be seen that using SBAS method, land subsidence can be extracted with the accuracy of sub-centimetre, even in the absence of ground control points. Comparing with ALOS data, Envisat data is more sensitive to the atmospheric change.

Acknowledgements
This study was supported by China National Science Fund (No. 41074019). JAXA has supplied the ALOS PALSAR data, and ESA has supplied the ENVISAT ASAR data. StaMPS software is used for taking DInSAR processing.

References

[1] XUE Yuqun, WU Jichun, ZHANG Yun, et al.. 2008. Simulation of land subsidence in Yangtze River delta. Science in China (D): earth science, pp. 477-492.(in Chinese)
[2] C. Prati, F. Rocca, and A. Monti Guarnieri, 1992. SAR interferometry experiments with ERS-1. Proc.1st ERS-1 Symp. Cannes, France, pp. 211-218.
[3] C. Prati, A. Ferretti, D. Perssin, 2010. Recent advance on surface ground deformation measurement by means of repeated space-borne SAR observations. Journal of Geodynamics, 49, pp. 161-170.
[4] D. Massonnet and K. L. Feigl, 1998. Radar Interferometry and its application to changes in the earth's surface. Reviews of Geophysics, 36 (4), pp. 441-500.
[5] Rosen, P. A., et al., 2000. Synthetic aperture radar interferometry. IEEE, pp. 333-328.
[6] Joaquin M S, Ramon H, Bert M K, Adele F, Nico A, 2003. Physical analysis of atmospheric delay signal observed in stacked radar interferometric data. IEEE, pp. 2112-2115.
[7] Ferretti, A., C. Prati and F. Rocca, 2001. Permanent Scatterers in SAR interferometry. IEEE TRANS. Geoscience and Remote Sensoring, 39.
[8] Berardino P., 2002. A New Algorithm for Surface Deformation Monitoring Based on Small Baseline Differential SAR Interferograms, IEEE Transactions on Geoscience and Remote Sensing, 40.
[9] Antonio Pepe, Mariarosaria Manzo, et al., 2008. Surface deformation of active volcanic areas retrieved with the SBAS-DInSAR technique: an overview. Annals of Geophysics, 51(1).
[10] R. F. Hanssen, 2001. Radar Interferometry: Data Interpretation and Error Analysis. Kluwer Academic Publishers, Dordercht, the Netherlands.
[11] D. Massonnet and K. L. Feigl, 1998. Radar Interferometry and its application to changes in the earth's surface. Reviews of Geophysics, 36 (4), pp. 441-500.
[12] T. G. Farr, M. Kobrick, 2000. Shuttle Radar Topography Mission produces a wealth of data, EOS Trans. AGU, Vol. 81, pp. 583-585.
[13] Shanghai geological environmental bulletin(2008), 1-13. 2009.05. (in Chinese)